Richardson-Lucy deconvolution for super-resolution imaging in a confocal microscope with programmable illumination

Author: Artem Trofymchuk

Facultat de Física, Universitat de Barcelona, Diagonal 645, 08028 Barcelona, Spain.

Advisor: Mario Montes Usategui

Abstract: I have tried a Richardson-Lucy deconvolution algorithm with a simulator of a programmable illumination laser microscope coded in Python for different excitation patterns, concluding that the most resolutive optimization process is for the multi point mode scanning, achieving a resolution below 100nm for a simulated noisy image.

I. INTRODUCTION

Fluorescence Confocal Microscopy has become a widely used tool in microscopic imaging, especially in research, where information from biological tissue images is of big interest. But, as it is well known, this is a diffraction-limited optical imaging system that for visible light has a resolution limit between 200nm and 350nm. Everything achieved below this resolution limit is usually understood as super-resolution microscopy. The feat to pass this limit was recognized in 2014 when the Nobel Prize of Chemistry was awarded to Eric Betzig, Stefan W. Hell, and William E. Moerner for the "Super-Resolved Fluorescence Microscopy" [1].

In the past years, a lot of research has been done towards this direction and with the constant improvement of computational power and technology, many researchers opt for computational approaches and the use of deep learning techniques. H. Wang et al. show super-resolution results in fluorescence microscopy [2] and A. Small et al. discuss several "Fluorophore localization algorithms for super-resolution microscopy" [3] that rely on switchable fluorophores and powerful algorithmic techniques of position estimation, for instance. In this FGW ("Final Grade Work") we implement a Richardson-Lucy deconvolution algorithm explained in [4] and [5] using a computational tool written in Python developed in a previous FGW by Sara Lumbreras that simulates an innovative confocal technique called Superfast Confocal Microscopy through Enhanced Acusto-Optic Modulation (SCREAM) [6]. This innovative method developed by Mario Montes Usategui and his team from the Optical Trapping Lab - Grup de Biofotònica (BiOPT) allows the creation of any kind of excitation patterns using two orthogonal Acusto-optical deflectors and holography.

So, the purpose of this work is to apply a super-resolution algorithm for microscopy images in a simulated environment and to study the result obtained with different excitation patterns and casuistry.

———

*Electronic address: `atrofytr7@alumnes.ub.edu`

II. METHODS AND RESULTS

A. Simulator Functioning

Both, the simulator and the algorithm are programmed in Python, mostly using pytorch library because of the optimized speed of execution and the possibility and easy way of executing the script in a Graphic Processing Unit (GPU). As it will be shown further, running the script in the GPU results in a very large improvement in the execution time.

It will be explained the basic concept of the functioning of the simulator relevant for this work, for additional or more specific information, we refer the reader to the cited FGW [7].

Firstly, the script calculates the point spread function (PSF), defined as the transverse spatial variation of the amplitude of the image received at the detector plane when the lens is illuminated by a perfect point source [9]. Then the excitation pattern is generated. The excitation pattern is the result of the convolution of an illumination pattern with the PSF of the illumination system. This illumination pattern is programmable and can be any pattern desired where the point of laser illumination is represented by a pixel with value 1. Then the sample is excited, this physical phenomenon can be easily modeled mathematically as a point-wise product of the excitation pattern and the "ground truth". The "ground truth" is the image with perfect resolution of the reality that we want to obtain, that we want to see. From this point on, the "ground truth" will be referred to as GT. The next step is the convolution of the excited image with the observation PSF. And finally, the image is passed through a camera binning, taking into account the pixel size of the image acquisition system, for example, a CCD.

This process is done in an arbitrary number of steps. If it is used, for example, an excitation pattern that is a grid of points separated some distance, and the sample is scanned with 16 steps displacing the points in the y-axis and then displacing them 16 steps in the x-axis, the result will be a stack of 256 images. One for every step. If the scanning is done first with straight lines in the x-axis with 16 steps and then with straight lines in the y-axis with the same amount of steps, the stack will have 32

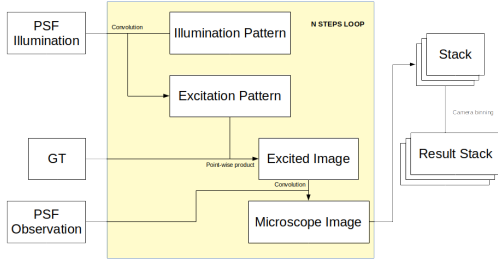images. Then, as an example, this stack can be collapsed

FIG. 1: Data flow representation of the simulator process

into a 2D image calculating the mean value of every pixel along the z-axis.

The operation flow is shown in FIG[1].

B. Richardson-Lucy Deconvolution Algorithm

An experimental image losses quality because of the convolution with the optical system PSF and the noise. The idea of the deconvolution algorithm is to invert the operation. But the operation in the other way is not as simple as it could seem. In [4] and [5] the following idea and algorithm are proposed:

A low-resolution image, m, can be considered as a high-resolution image, d, degraded because of the multiplication with a matrix, H, that represents a downgrading process and the addition of a possible background signal, b.

$$m = Hd + b \qquad (1)$$

In this particular case, H is the simulation, the imaging process. It is the measurement itself that involves the steps explained in the previous subsection.

As it is known, real fluorescence microscopy measurements have always noise due to the limitations of electronic detectors. Adapting the Equation (1) to a noisy image measurement is obtained the Equation (2):

$$m_n = P(Hd + b) \qquad (2)$$

where m_n is the noisy low-resolution image and P represents the addition of Poisson noise.

The starting point for the algorithm is an initial estimate of the high-resolution image. In this FGW we always used as the initial guess the result of collapsing the stack of images given by the simulation code into an image summing up the images along the z-axis, considering the XY plane as the image obtained in every iteration.

The algorithm to enhance the initially estimated image into a super-resolved one is the following iterative process (see [4] & [5] for details):

$$m = He_i + b \qquad (3)$$

$$r = m_n/m \qquad (4)$$
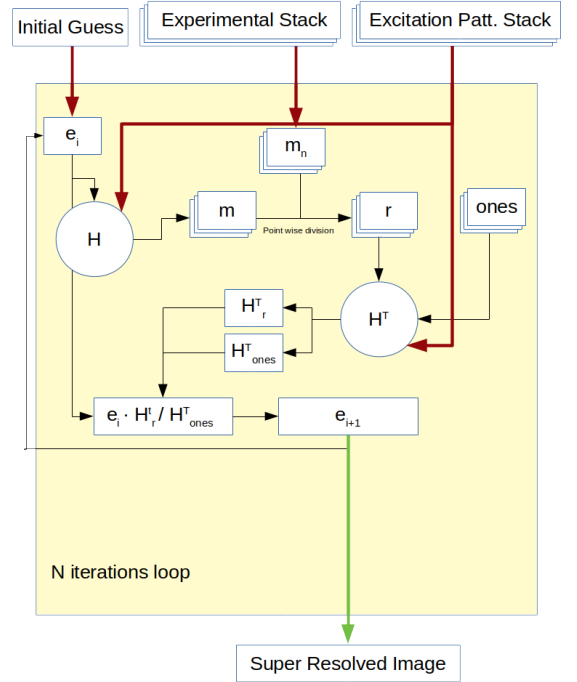
$$e_{i+1} = e_i H^T r / H^T ones \qquad (5)$$

FIG. 2: Data flow representation of the image enhancement algorithm. Red lines represent the input arguments and green lines represent the final output of the algorithm after N arbitrary number of iterations

Here, the estimated image that we want to upgrade, and that is the output of the algorithm is represented as e_i, and H^T is the transpose of the measurement matrix H. In the same way as it is explained in [6] we implemented H^T reversing the order of operation of the imaging process. Considering this, $H^T r$ and $H^T ones$ is understood as the application of H to r and a matrix with all the values equal to one. So if we had:

$$H = (EP_{stack} image) * PSF \qquad (6)$$

Where EP_{stack} represents all the stack of excitation patterns because H represents all the measurements. H^T becomes into:

$$H^T = (image_{stack} * PSF) EP_{stack} \qquad (7)$$

Note that the order of operation is from left to right, being the point wise product the first operation in H and the convolution in H^T. In the Equation (6) and Equation (7) it is possible to observe that H takes an image as

input and returns a stack of observations and that H^T does the contrary, takes as input the stack, and returns an image that is calculated summing the resulting stack in the z-axis.

C.   Results

As it was explained before, in both tools, the SCREAM system and the simulator, exists the possibility of illuminating the sample with a completely arbitrary pattern. To proof the super resolution capability of the studied approach, we generated different simulated data and compared the efficiency of the algorithm itself and the efficiency of the illumination modes explained below.

- Multi Points: Consists in a grid of points that move along the x and y-axis consecutively the number of times that it is defined with the number of steps parameter. So if it is defined n number of steps, it will generate a stack of $n * n$ frames.

- Random: Consists in a random pattern for every step. The result is a stack of n frames.

- Multi line xy: It is a combination of the modes multi line x and y that consists in straight lines along one axis. Firstly, is done the scanning horizontally and then vertically, as an example. It results in a stack with $n + n$ frames.
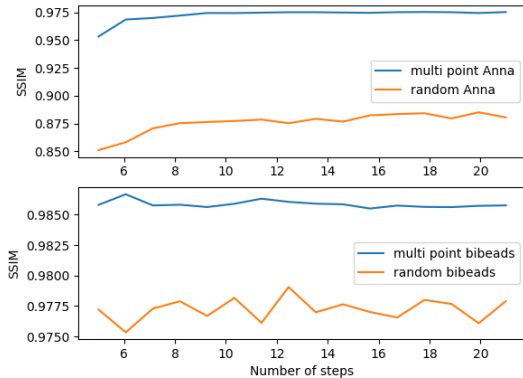

FIG. 3: Representation of the effect of scanning with more steps. Algorithms applied to "Anna Palm" and "Bibeads"[a] images

[a]"Bibeads" image is a simulated image that generates a set of point emitters grouped in pairs with a certain distance between the centers of the points

Also, for the scanning were used the following system parameters: A laser illumination with a $523nm$ wavelength, microscope objective with $NA = 1.2$, an effective pixel size of $10nm$, and a camera binning of $40nm$.

To help better understanding of the resolution improvement done it was decided to quantify it with the
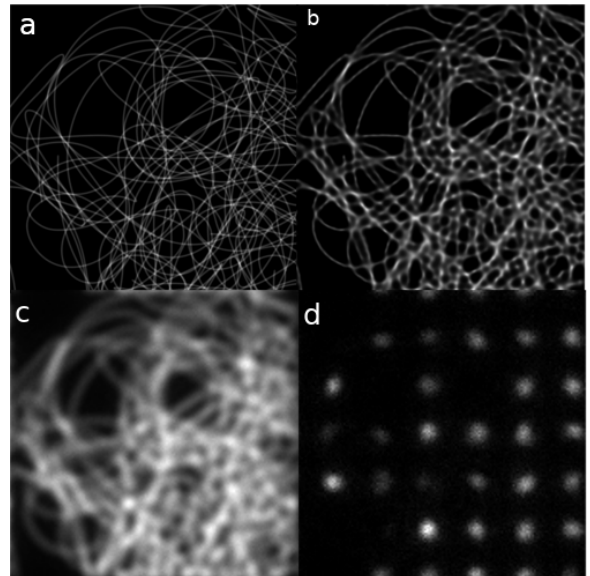

FIG. 4: Obtained results of the scanning of "Anna Palm" image with multi point illumination mode and 500 iterations. a, b, c, d are the GT, the super-resolution image (SR), the epi-fluorescence image (EPI) and, a frame from the experimental stack, respectively. 0.53 SSIM achieved in 423.6s.
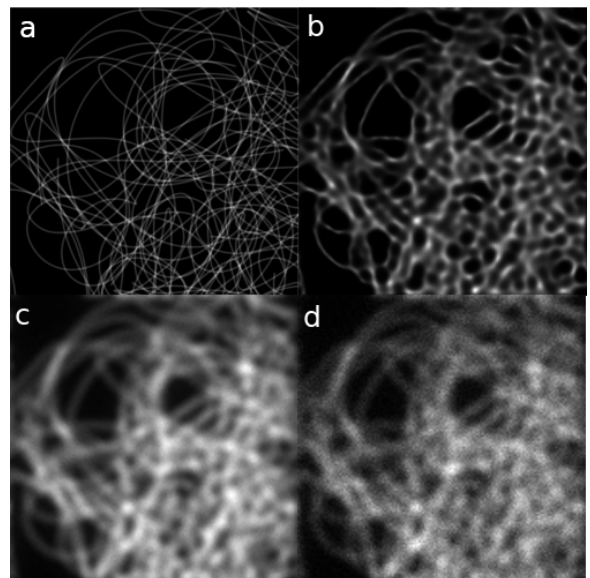

FIG. 5: Obtained results of the scanning of "Anna Palm" image with random illumination mode with 16 steps and optimization with 500 iterations. a, b, c, d are the GT, the SR image, the EPI and, a frame from the experimental stack, respectively. 0.32 SSIM achieved in 58.28s.

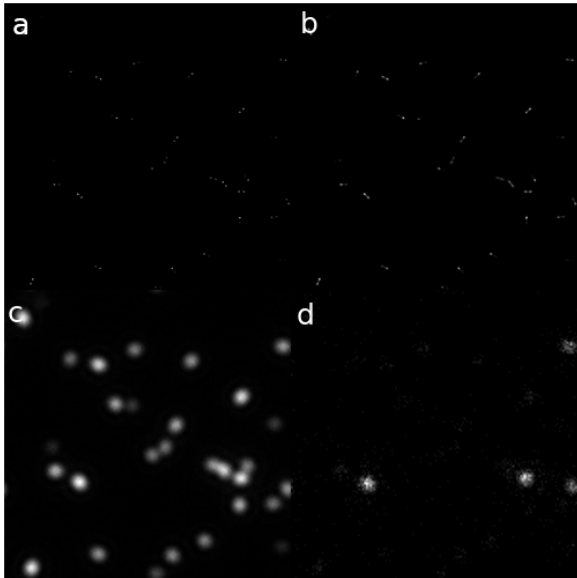structure similarity value (SSIM) calculated between the GT and SR images. [10]

FIG. 6: Scanning of "Bibeads" with a distance of 100nm between centers and blurred in x and y directions with a gaussian filter with a std of 20nm. Scanning done with 16 steps multi point mode and 500 iterations.a, b, c, d are the GT, the SR image,the EPI and, a frame from the experimental stack, respectively. 0.9926 SSIM achieved in 455,6 s
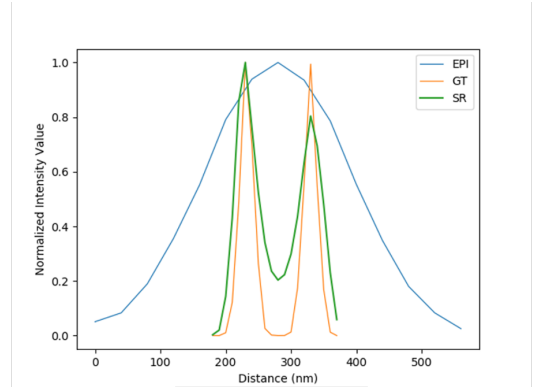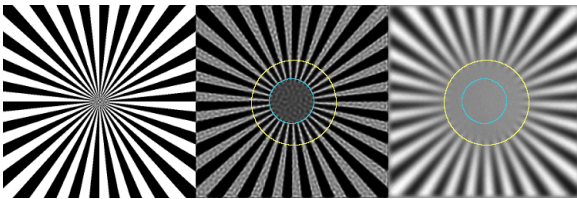

FIG. 7: Obtained results of the scanning and optimization of Siemens Star resolution test image with 16 steps in multi point mode and 2000 iterations. From left to right are represented the GT, the SR image and, the EPI. Yellow and blue circles represent the visual resolution limit of the EPI and the SR, respectively, showing that the resolution approximately is improved by a factor 2
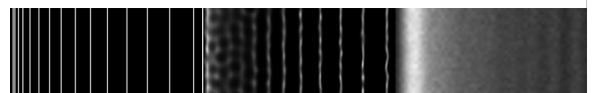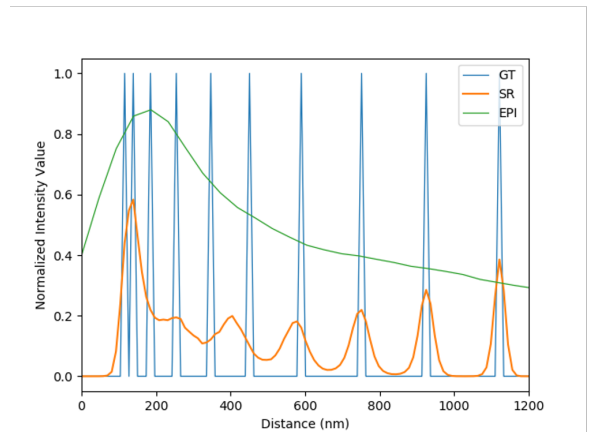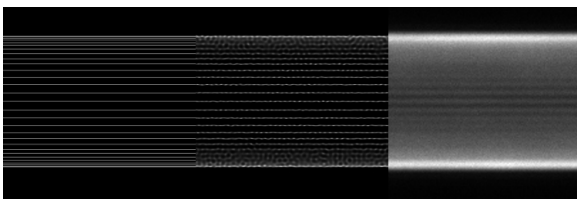

FIG. 8: Obtained results of the scanning and optimization of the lines resolution test image with 16 steps in multi point mode and 2000 iterations. From left to right are represented the GT, the SR image and, the EPI.

III. CONCLUSIONS

We have seen, from the results of the experiments, that the addition of steps for the scanning does not result in a

FIG. 9: Intensity profile of GT, SR image and EPI of the "Bibeads" zoomed image, from left to right order. 100nm distance between the centers of the points

FIG. 10: Intensity profile of GT, SR image and EPI of the "Lines Test" image calculated over 600 different line profiles. From left to right order.

significant improvement. Actually, some improvement is only seen in images with a bigger density of information, as "Anna Palm". In images of a low level of information as "Bibeads" there is no clear improvement obtained (FIG[3]). Also, the addition of steps increases the computational capability and time needed to optimize the resolution for a visual improvement that is practically not perceptible. For example, the difference of time between scanning in multi point mode of 5 and 20 steps is bigger than a factor of 8 because of the quadratic depen-

IMAGE	IL.MODE	TIME(s)	SSIM
Anna Palm	random	47.24	0.2402
	multi point	44.43	0.3879
	multi line xy	44.09	0.2986
Bibeads 240nm	random	23.46	0.9026
	multi point	21.55	0.9474
	multi line xy	21.24	0.9330
Siemens Star	random	24.52	0.0921
	multi point	18.12	0.1414
	multi line xy	20.56	0.1142
Lines	random	24.18	0.0088
	multi point	20.49	0.0246
	multi line xy	20.46	0.0148

TABLE I: Comparison of execution times and achieved SSIM between illumination modes for different simulated images in the same conditions. Executed with a scanning resulting in 36 frames and an optimization of 50 iterations

DEVICE	IL.MODE	TIME(s)
GPU	random	1.91
	multi point	14.51
	multi line xy	2.87
CPU	random	15.13
	multi point	91.31
	multi line xy	17.87

TABLE II: Comparison of execution times between GPU and CPU for a scanning of 16 steps and an optimization of 50 iteration done to the same simulated image

dence of the number of frames with the number of steps. For a random illumination mode is more than a 1.5 times slower with 20 steps than with 5, because of the linear relation between the number of steps and frames. Although, from the TABLE[1] and FIG[3] we can see that the maximum SSIM values are achieved with multi point illumination mode. Certainly, according to the needed resolution and execution times, the other modes can be really useful and of big interest because of the much faster optimization if few steps are used, and even though decent SSIM achieved values. That decreases the photobleaching problem because of illuminating fewer times the same point in the sample.

The obvious computational power superiority of a GPU with 3840 cores and 12 GB of memory over a Central Processing Unit (CPU) of 8 GB of memory and 4 cores, can be easily concluded from the execution times showed in TABLE[2].

Hence, we opted to use 16 steps to demonstrate the resolution capability of the algorithm. We can affirm, considering the results shown in FIG[4][5][6] that the algorithm approach is successful, achieving resolutions below 100nm (FIG[9]). The visual quality increase of the images is undoubtful. To be able to quantify the resolution power, "Siemens Star" and "Lines" resolution test images were used and from the intensity profile analysis, we can declare an achieved resolution below 150nm (FIG[7][8][10]).

Acknowledgments

[1] Royal, T. H. E., Academy, S., Sciences, O. F. (2014). Nobel Prize ℝ Scientific Backgroumd Article. 50005. https://www.nobelprize.org/prizes/chemistry/2014/advanced-information/

[2] Wang, H., Rivenson, Y., Jin, Y., Wei, Z., Gao, R., Günaydin, H., Bentolila, L. A., Ozcan, A. (2018). Deep learning achieves super-resolution in fluorescence microscopy. BioRxiv, 1–29. https://doi.org/10.1101/309641

[3] Small, A., Stahlheber, S. (2014). Fluorophore localization algorithms for super-resolution microscopy. Nature Methods, 11(3), 267–279. https://doi.org/10.1038/nmeth.2844

[4] Ingaramo, M., York, A. G., Hoogendoorn, E., Postma, M., Shroff, H., Patterson, G. H. (2014). Richardson-Lucy deconvolution as a general tool for combining images with complementary strengths. ChemPhysChem, 15(4), 794–800. https://doi.org/10.1002/cphc.201300831

[5] Ströhl, F., Kaminski, C. F. (2015). A joint Richardson-Lucy deconvolution algorithm for the reconstruction of multifocal structured illumination microscopy data. Methods and Applications in Fluorescence, 3(1). https://doi.org/10.1088/2050-6120/3/1/014002

[6] M. Montes Usategui, R. Bola, E. Martín Badosa and D. Treptow, "Programmable multi-point illuminator, confocal filter, confocal microscope and method to operate said confocal microscope". Patent WO/2020/007761

[7] Barcelona, U. De. (n.d.). Development of a computational tool for a new fluorescence microscopy technique. http://hdl.handle.net/2445/141527

[8] Ouyang, W., Aristov, A., Lelek, M. et al. Deep learning massively accelerates super-resolution localization microscopy. Nat Biotechnol 36, 460–468 (2018). https://doi.org.sire.ub.edu/10.1038/nbt.4106

[9] Timothy R. Corle, Gordon S. Kino, in Confocal Scanning Optical Microscopy and Related Imaging Systems, 1996

[10] Zhou Wang, Member, Alan Conrad Bovik et al. Image Quality Assessment: From Error Visibility to Structural Similarity DOI 10.1109/TIP.2003.819861